MOLECULAR
METABOLISM

Essential roles of insulin and IGF-1 receptors during embryonic lineage development

Erin R. Okawa [1,2,5,6], Manoj K. Gupta [1,5], Sevim Kahraman [1], Praneeth Goli [1], Masaji Sakaguchi [1], Jiang Hu [1], Kaiti Duan [1], Brittany Slipp [1], Jochen K. Lennerz [3], Rohit N. Kulkarni [1,4,*]

ABSTRACT

The insulin and insulin-like growth factor-1 (IGF-1) receptors are important for the growth and development of embryonic tissues. To directly define their roles in the maintenance of pluripotency and differentiation of stem cells, we knocked out both receptors in induced pluripotent stem cells (iPSCs). iPSCs lacking both insulin and IGF-1 receptors (double knockout, DKO) exhibited preserved pluripotency potential despite decreased expression of transcription factors *Lin28a* and *Tbx3* compared to control iPSCs. While embryoid body and teratoma assays revealed an intact ability of DKO iPSCs to form all three germ layers, the latter were composed of primitive neuroectodermal tumor-like cells in the DKO group. RNA-seq analyses of control vs DKO iPSCs revealed differential regulation of pluripotency, developmental, E2F1, and apoptosis pathways. Signaling analyses pointed to downregulation of the AKT/mTOR pathway and upregulation of the STAT3 pathway in DKO iPSCs in the basal state and following stimulation with insulin/IGF-1. Directed differentiation toward the three lineages was dysregulated in DKO iPSCs, with significant downregulation of key markers (*Cebpα*, *Fas*, *Pparγ*, and *Fsp27*) in adipocytes and transcription factors (*Ngn3*, *Isl1*, *Pax6*, and *Neurod1*) in pancreatic endocrine progenitors. Furthermore, differentiated pancreatic endocrine progenitor cells from DKO iPSCs showed increased apoptosis. We conclude that insulin and insulin-like growth factor-1 receptors are indispensable for normal lineage development and perturbations in the function and signaling of these receptors leads to upregulation of alternative compensatory pathways to maintain pluripotency.

© 2021 The Authors. Published by Elsevier GmbH. This is an open access article under the CC BY-NC-ND license (http://creativecommons.org/licenses/by-nc-nd/4.0/).

Keywords Insulin/IGF-1 receptors; Pluripotency; Lineage development; Signaling; Apoptosis

1. INTRODUCTION

Insulin and insulin-like growth factor (IGF) receptors belong to a highly conserved family of receptors and ligands known to be involved in cell proliferation, metabolic signaling, and organogenesis [1—3]. Transcripts for the insulin receptor (IR) and IGF1 receptor (IGF1R) have been detected in unfertilized human oocytes and pre-implantation embryos at all stages, and both play important roles in embryogenesis [4]. Insulin is able to bind both receptors, can be detected in the fetal pancreas as early as 52 days post—conception, and acts in an endocrine manner [5]. IGF-1 and IGF-2, also detected in the first trimester, are produced by multiple organs and act in a growth hormone-independent endocrine, paracrine, or autocrine manner. Mice with a knockout of IR exhibit growth defects late in embryogenesis and are born ∼90% of normal birth weight [6]. In contrast, IGF1R knockout mice are 45% of normal birthweight and exhibit organ hypoplasia, ossification delays, central nervous system abnormalities and die immediately after birth due to respiratory failure [7]. Intriguingly, knockout of both receptors results in mice that are 30%

of normal birthweight but otherwise resemble IGF1R knockout mice [8]. These data point to a role of both receptors in early embryonic life. Upon binding of their ligands (insulin, IGF-1, or IGF-2), IR and IGF1R autophosphorylate and in turn phosphorylate insulin receptor substrates. These substrates become scaffolds for 2 major cellular signaling nodes: the phosphatidylinositol-3-kinase (P13K)-AKT/protein kinase B (PKB) pathway and mitogen-activated protein kinase (MAPK)/ERK pathway [9,10]. IGF1R also signals through the Janus kinase/signal transducer and activator of the transcription (JAK/STAT) pathway, particularly through STAT1 and STAT3 [11,12].

In both human and mouse embryonic stem cells (ESCs), the P13K pathway is important for maintenance of pluripotency, proliferation, and survival [13—17]. The MAPK/ERK pathway, however, appears to play different roles in human vs mouse ESCs. While human ESCs exhibit ERK signaling via fibroblast growth factor receptor (FGFR) [18], mouse ESCs require the inhibition of MEK signaling to maintain cells in a pluripotent state; additionally, reduced ERK signaling in mouse ESCs leads to genomic instability and telomere shortening [19,20].

The individual roles of IR and IGF1R have been studied in stem cell maintenance and differentiation. IR is important for self-renewal of *Drosophila* germline stem cells and maintaining pluripotency of mouse ESCs [21—24]. Our laboratory previously reported that IR-mediated signaling regulates pluripotency and lineage development in mouse iPSCs [25]. However, the downregulation of IR leads to defects in embryogenesis in zebrafish, suggesting that its expression is important for tissue differentiation [26].

IGF1R has been reported to be important for self-renewal and survival of human ESCs [27,28]. This is further supported by the finding that IGF1R is downregulated in human ESCs that undergo differentiation into hepatocytes [29]. Conversely, IGF1R activation is required for differentiation of rat bone marrow mesenchymal stem cells into cardiomyocyte-like cells. It has also been reported that suppressing IGF1R expression in mouse neural stem cells leads to maintenance of pluripotency and a stem-like state [30,31].

Considering that the activation of IR and IGF1R leads to multiple common downstream signaling proteins, we studied the consequences of a double knockout (DKO) of the two receptors on pluripotent stem cell lineage development and cell signaling. RNA-seq analyses, corroborated by signaling studies, revealed for the first time (to the best of our knowledge) that iPSCs lacking insulin/IGF-1 receptors are able to maintain pluripotency while defaulting toward a neuro-ectodermal lineage. These mutant iPSCs demonstrated skewed mesodermal (adipocyte) and endodermal (pancreatic) lineage development and manifested alterations in multiple signaling pathways.

2. MATERIALS AND METHODS

2.1. Mice and mouse embryonic fibroblasts (MEFs)
All of the animal experiments were approved by the Institutional Animal Care and Use Committee of the Joslin Diabetes Center. MEFs were derived from double-floxed IR/IGF1R embryonic day 13.5 fetuses; the mice came from a C57/Bl6 background. The fetuses were washed twice with 1x Dulbecco's phosphate-buffered saline (DPBS) (Thermo Fisher Scientific) and their heads and livers were removed before maceration and digestion with Trypsin—EDTA (Invitrogen). All of the MEFs were cultured at 37°C in 5% CO_2 and maintained in Dulbecco's Modified Eagle's Medium (DMEM) supplemented with 10% fetal bovine serum, 1% non-essential amino acids, and 1% penicillin/streptomycin. The media was changed every other day. MEFs were maintained up to a maximum passage of 5.

2.2. Adenoviral-mediated double knockout (DKO) of IR and IGF1R
MEFs were cultured in media as previously described. Ad5CMVCre and Ad5CMVeGFP (University of Iowa Viral Vector Core Facility, Iowa City, IA, USA) were thawed and added to MEF media along with polybrene (Santa Cruz Biotechnology); after 24 hours, the MEFs were washed with 1x Dulbecco's phosphate-buffered saline (DPBS) (Thermo Fisher Scientific) and fresh media was added. GFP fluorescence was visualized using a fluorescence microscope.

2.3. Lentiviral mediated reprogramming and induced pluripotent stem cell (iPSC) generation and characterization
Reprogramming was performed on DKO and control MEFs using a mouse STEMCCA lentiviral vector expressing *Oct4*, *Sox2*, *Klf4*, and *cMyc*. In brief, MEFs were grown in MEF media as previously described. Then 200 uL of STEMCCA vector and 1 uL of polybrene (Santa Cruz Biotechnology) were added to each well. After 24 hours, the cells were washed with DPBS and the media changed to ESC media DMEM supplemented with 15% FBS, 1 u/mL of leukemia inhibitory factor (LIF) (Millipore), 1% non-essential amino acids, and 1% penicillin/streptomycin. After 10—14 days, individual iPSC colonies were isolated and expanded on irradiated MEFs grown on gelatin-coated plates. We selected 4 individual iPSC clones from DKO MEFs and 4 individual iPSC clones from control MEFs.

2.4. IPSC studies
IPSCs were initially maintained on irradiated MEFs (MTI-GlobalStem) in media as previously described. For experimentation, iPSCs were exposed to Accutase (Stem Cell Technology) to aid in detachment from irradiated MEFs and plated onto gelatin-coated plates. The media was changed to ESGRO 2i media (Millipore) and the cells were passaged every other day for 1 week to deplete irradiated MEFs.

Alkaline phosphatase staining was performed after the cells were fixed with 10% neutral buffered formalin solution (Wako). Basal iPSC experiments were performed after iPSCs were grown for 16 hours in DMEM high-glucose, high-pyruvate media supplemented with 0.1% BSA (Wako) and 1 unit/mL of LIF (Millipore). For iPSC signaling experiments, cells were split and seeded at a density of 2×10^5 onto gelatin-coated 6-well plates. Cells were grown in DMEM/F-12 media with 1 unit/mL of LIF (Millipore) for 16 hours. Then 100 nM of insulin (Sigma—Aldrich), 100 nM of IGF1 (Sigma—Aldrich), or 100 units/mL of LIF (Millipore) were added to each well for 15 min.

2.5. Embryoid body formation
Control and DKO iPSCs grown in 2i media were collected after Accutase (Stem Cell Technology) treatment and 2×10^6 cells were placed in 10 cm petri dishes and grown in DMEM media supplemented with 20% FBS, 1% non-essential amino acids, and 1% penicillin/streptomycin. The media was changed every other day. After 10 days, embryoid bodies were collected via centrifugation. We used a spontaneous method of EB production rather than the hanging drop method to enable a larger yield of EBs.

2.6. Teratoma formation
Control and DKO iPSCs grown in 2i media were collected after Accutase (Stem Cell Technology) treatment and resuspended in Matrigel (Thermo Fisher Scientific). Then 1×10^6 cells were injected both intramuscularly and subcutaneously into NOD-SCID mice. Palpable tumors were observed 2 weeks after injection. Tumor samples were collected after 4 weeks, fixed in 10% formalin, and processed for paraffin embedding and sectioning. Hematoxylin and eosin staining and immunostaining of teratoma sections was performed using antibodies.

2.7. Neuronal differentiation
Control and DKO iPSCs grown in a 2i system were collected using Accutase (Stem Cell Technology). Then 1.5×10^5 control and DKO iPSCs were plated in triplicate onto gelatin-coated 6-well plates and differentiated up to 10 days in Ndiff 227 media (Clontech) [38]. Cells were harvested on day 10 for transcript analyses of neuronal markers; immunostaining was also performed using antibodies directed toward nestin (ab7659, Abcam), N-cadherin (ab18203, Abcam), β-III-tubulin (ab52901, Abcam), and synaptophysin (ab14692, Abcam).

2.8. Adipocyte differentiation
Control and DKO iPSCs were differentiated into adipocytes using a slightly modified protocol from [41]. The protocol allows iPSCs to differentiate into adipocytes for 27 days in response to a combination of cocktails at various steps. The adipocytes were subjected to Oil Red O staining for confirmation of lipid droplets. Total RNA was isolated for transcript analyses of adipocyte markers.
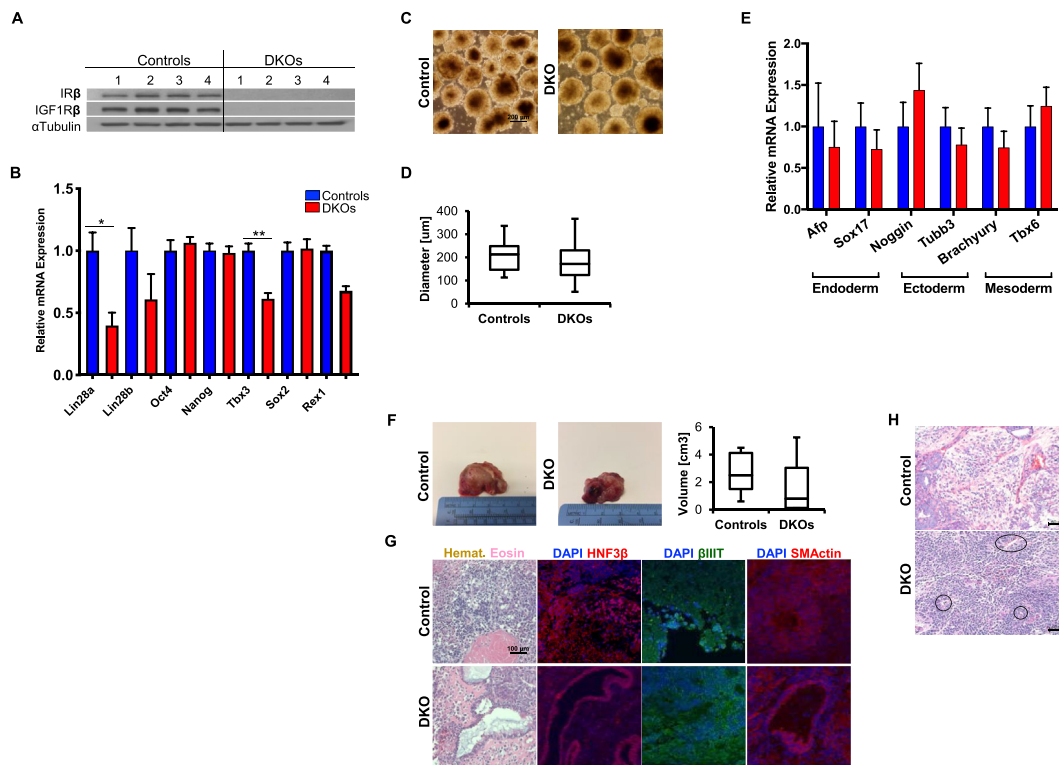
Figure 1: DKO iPSCs sustained the ability to maintain pluripotency in vitro and in vivo and formed neuroectodermal tumor-like cells during in vivo differentiation. (A) Immunoblotting for IR and IGF1R in MEFs; α-tubulin served as a loading control. Protein levels of both receptors were virtually undetectable in DKO MEFs. (B) Relative gene expression analyzed by qRT-PCR for *Lin28a*, *Lin28b*, *Oct4*, *Nanog*, *Tbx3*, *Sox2*, and *Rex1* in control (blue) and DKO (red) iPSCs. Gene expression levels were normalized to *Gapdh*, and DKO expression was normalized to controls using the comparative threshold cycle (ΔΔCT) method. Data represent the mean ± SEM (n = 3). Statistical analysis via Student's *t*-test. *p < 0.05 and **p < 0.005. (C) Representative microscopic images of embryoid bodies on day 10 (magnification 20x). (D) Mean diameter (in μm) of embryoid bodies (n = 3). (E) Relative gene expression analyzed by qRT-PCR of lineage markers *Afp*, *Sox17*, *Noggin*, *Tubb3*, *Brachyury*, and *Tbx6* in control and DKO embryoid bodies. *Afp* and *Sox17* are markers of endoderm, *Noggin* and *Tubb3* are markers of ectoderm, and *Brachyury* and *Tbx6* are markers of mesoderm. Gene expression levels were normalized to *Gapdh*, and DKO expression was normalized to controls using the comparative threshold cycle (ΔΔCT) method. Data represent the mean ± SEM (n = 3). (F) Representative photographs of control and DKO teratomas. Teratoma dimensions were not statistically different between control and DKOs. (G) Representative hematoxylin and eosin stained images of control and DKO teratomas. Immunohistochemistry of teratomas for markers of endoderm (HNF-3β), ectoderm (β-III-tubulin), and mesoderm (α-smooth muscle actin). Nuclei stained with DAPI are in blue. (H) Representative hematoxylin and eosin stained control and DKO teratomas showing an unusual primitive neuroectodermal tumor phenotype in DKOs (circled).

2.9. Pancreatic endocrine progenitor cell differentiation

Control and DKO iPSCs were differentiated into pancreatic endocrine progenitor cells using a protocol from [44,45]. Pancreatic endocrine progenitor cells were obtained on days 5 and 10. Total RNA was isolated from day 5 and day 10 differentiated cells for transcript analyses of beta cell developmental markers. Differentiated cells were immunostained for Pax6 (ab5790, Abcam), Isl1 (ab20670, Abcam), and neurogenin 3 (F25A1B3, Developmental Studies Hybridoma Bank, DSHB).

2.10. Analysis of cell proliferation

IPSCs were plated in 96-well plates with 10^4 cells in each well. Cell numbers were determined using a CellTiter 96 Non-Radioactive Cell Proliferation Assay (Promega, G4001) per the manufacturer's protocol.

2.11. RNA analysis and qRT-PCR

RNA isolation and cDNA synthesis were performed as previously described [62]. The primers described in Table S1 were used for amplification.

2.12. Immunoblotting

Cells were solubilized in M-PER lysis buffer (Thermo Fisher Scientific) with protease inhibitors and phosphatase inhibitors (Sigma—Aldrich) and the protein concentration was measured using a BCA protein assay kit (Pierce). The extracts were subjected to Western blotting with primary antibodies overnight at 4°C. The following antibodies from Cell Signaling Technology were utilized: anti-AKT (#9272S), anti-β-actin (#4967S), anti-ERK5 (#3372S), anti-Gapdh (#5174S), anti-Igf1r (#9750S), anti-Irβ (#3025S), anti-mTOR (#2983S), anti-Nanog (#8822S), anti-Oct4 (#2750S), anti-p44/42 MAPK (#9102S), anti-phospho-AKT (#4060S), anti-phospho-mTOR (#5536S), anti-phospho-p44/42 MAPK (#4377S), anti-phospho-STAT3 (#9145S), and anti-Sox2 (#23064S). Anti-α-tubulin (ab7291), anti-α-smooth muscle actin (ab32575), anti-β-III tubulin (ab52901), anti-LIFR (ab101228), anti-Lin28 (ab46020), anti-N-cadherin (ab18203), anti-nestin (ab7659), and anti-Tbx3 (ab99302) were from Abcam. Anti-actin (sc-1616), anti-Hnf3β (sc-374,376), anti-STAT3 (sc-482), anti-rabbit IgG (sc-2054), and anti-mouse IgG (sc-2055) were from Santa Cruz Biotechnology. Alexa Fluor 488 goat anti-mouse IgG (A11001), Alexa Fluor 488 goat anti-rabbit IgG (A11008), and Alexa Fluor 546 goat anti-rabbit IgG (A11010) were from Invitrogen. Densitometry was performed using ImageJ software.

2.13. Histology and immunostaining

IPSCs were fixed in 4% paraformaldehyde solution (Wako) prior to staining with specific primary antibodies. Teratoma sections were fixed in paraformaldehyde, processed, and embedded in paraffin. All of the
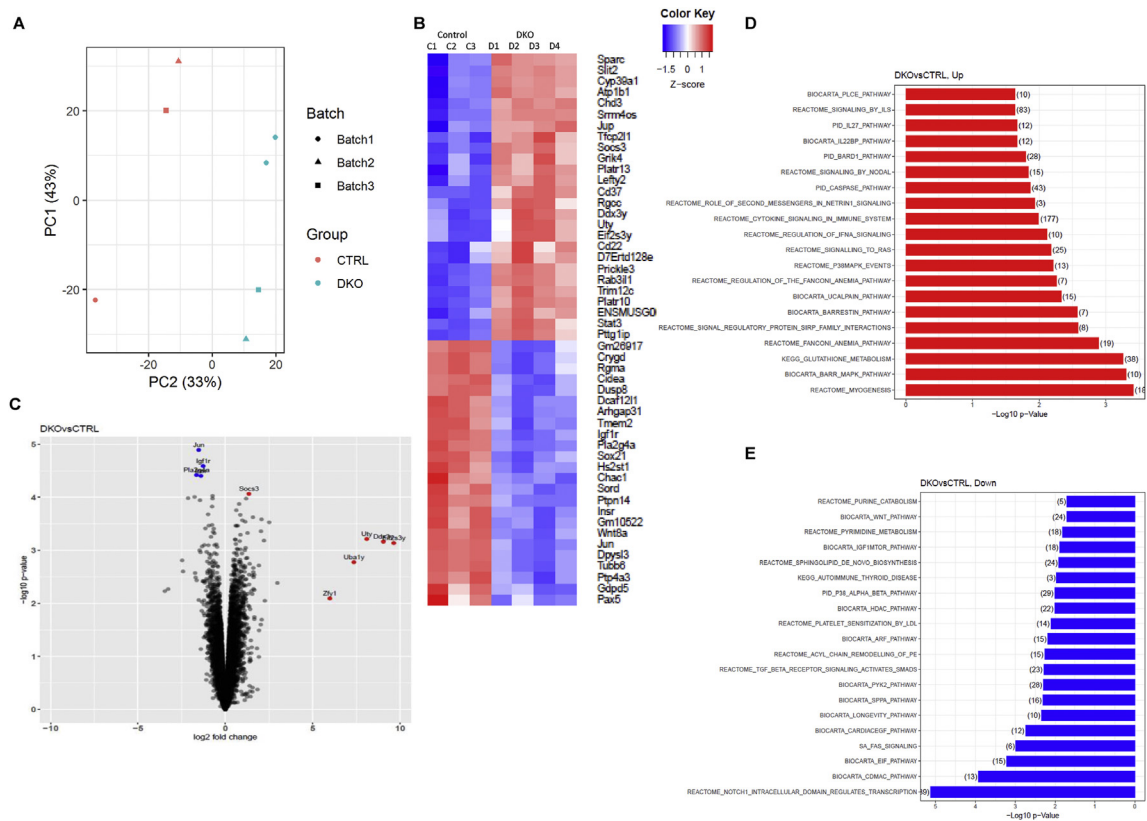
Figure 2: RNA sequencing analysis of control vs DKO iPSCs showed upregulation of E2F1 (apoptosis) and JAK-STAT pathways in DKO iPSCs. (A) PCA plot of control and DKO iPSCs. (B) Heat map depicting top upregulated (red) and downregulated (blue) genes; control vs DKO iPSC clones. (C) Volcano plot of RNA sequencing data comparing DKO vs control iPSC clone gene expression. Genes that were upregulated (n = 6) by twofold or more and with a p value < 0.05 are depicted as red dots, and genes that were downregulated (n = 4) by fourfold or more and with a p value < 0.05 are depicted as blue dots. (D) Canonical pathway analysis assessing the most upregulated pathways in DKO vs control iPSC clones. (E) Canonical pathway analysis assessing the most downregulated pathways in DKO vs control iPSC clones.

sectioning and histopathology procedures were performed at the DF/HCC Research Pathology Core. Slides were analyzed by hematoxylin and eosin staining or immunostaining with specific primary antibodies.

3. QUANTIFICATION AND STATISTICAL ANALYSIS

3.1. Statistics

All of the experiments were independently repeated at least three times, and all of the results are shown as mean ± SEM. Statistical comparisons between groups were analyzed for significance by unpaired two-tailed Student's *t*-test and two-way ANOVA with multiple Tukey's tests. Differences were considered significant if p < 0.05. The values of *n*, statistical measures (mean ± SEM), and statistical significance are reported in the figures and figure legends.

4. RESULTS

4.1. Induced pluripotent stem cells (iPSCs) with a double knockout (DKO) of IR and IGF1R maintained their pluripotent potential and formed primitive neuroectodermal tumor-like cells in teratomas in vivo

We obtained mouse embryonic fibroblasts (MEFs) from 4 mouse embryos (embryonic E-day 13.5) extracted from 4 female C57Bl/6 mice expressing floxed sites for exon 4 of IR and exon 3 of IGF1R (Figure S1A). To knock down the receptors, cultured fibroblasts were infected with either an Ad5CMVCre or Ad5CMVGFP (control) vector. Knockout of IR or

IGF1R was assessed by qRT-PCR (n = 4); MEFs exposed to Ad5CMVCre showed a 79−96% reduction in IR and 80−97% reduction in IGF1R compared to MEFs exposed to Ad5CMVGFP (Figure S1B). To create the iPSCs, we reprogrammed the DKO MEFs with a STEMCCA lentiviral vector [32]. Interestingly, reprogramming efficiency decreased by ∼73% in DKO MEFs compared to control MEFs (Figure S1C). Considering that knocking down only IR does not significantly impact reprogramming efficiency [25], further studies are warranted to directly address the relevance of IGF1R signaling in reprogramming.

After confirming the knockdown of IR and IGF1R by immunoblotting we cultured and further characterized individual iPSC clones (DKOs and controls, n = 4 each) (Figure 1A). Evaluation of key pluripotency markers (*Lin28a*, *Lin28b*, *Oct4*, *Nanog*, *Tbx3*, *Sox2* and *Rex1*) using qRT-PCR revealed a 60% downregulation of *Lin28a* (p < 0.05) and a 38% decrease in *Tbx3* (p < 0.005) gene expression in DKO iPSCs compared to controls (Figure 1B).

We subsequently generated embryoid bodies to assess the ability of either DKO or control iPSCs to spontaneously differentiate in vitro. Both groups displayed embryoid bodies with similar sizes after 10 days of culture (control, 205 μm vs DKOs, 181 μm) (Figure 1C,D). We also assessed the ability of embryoid bodies to spontaneously differentiate into derivatives of the 3 germ layers. Quantitative RT-PCR analysis showed no significant difference in the expression of the endodermal (*Afp* and *Sox17*), ectodermal (*Noggin* and *Tubb3*), and mesodermal (*Brachyury* and *Tbx6*) markers between the control and DKO embryoid bodies (Figure 1E).
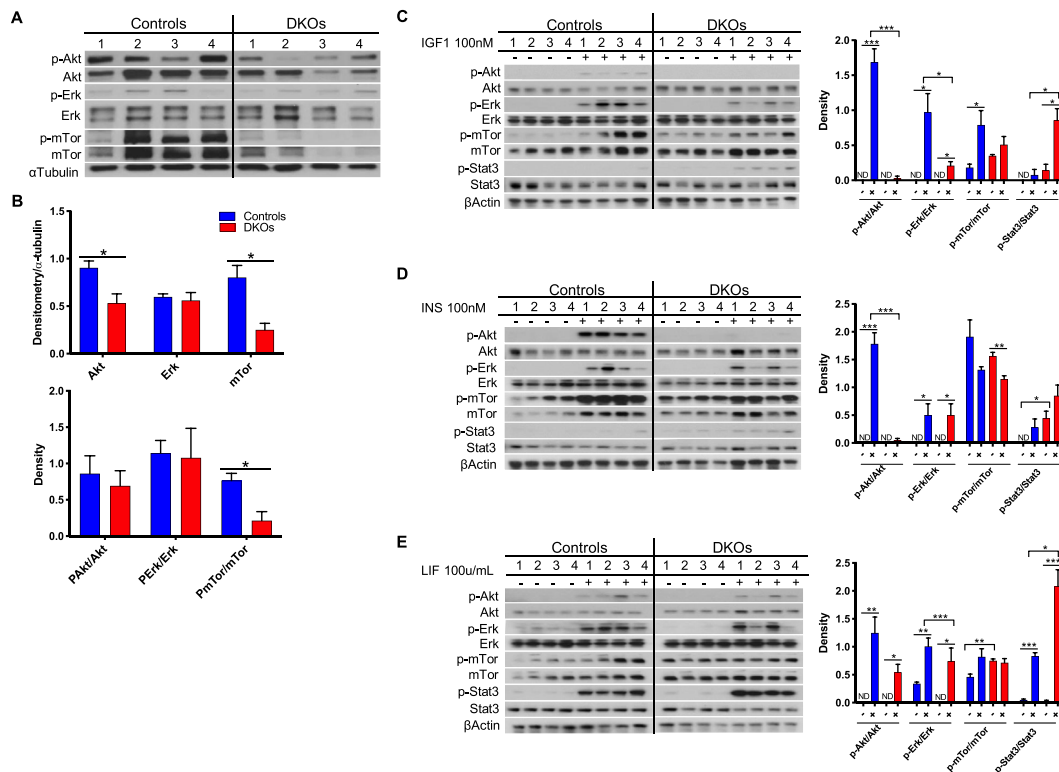
Figure 3: P13K/Akt signaling was downregulated while the STAT3 pathway was upregulated in DKO iPSCs. (A) Immunoblotting of signaling proteins p-AKT, AKT, p-ERK, ERK, p-mTOR, and mTOR in control and DKO iPSCs grown for 24 hours in basal media (DMEM + 0.1% BSA); α-tubulin served as a loading control. (B) Quantification of total AKT, ERK, and mTOR protein was performed by normalizing total protein values against α-tubulin values using densitometry. Quantification of phosphorylation was performed by normalizing phosphorylation values against total protein values using densitometry. Data represent the mean ± SEM. *$p < 0.05$ and ***$p < 0.0005$. (C) Left: Immunoblotting of signaling proteins in control and DKO iPSCs grown for 24 hours in basal media that were stimulated with 100 nM IGF1 for 15 min; β-actin served as a loading control. Right: Quantification of phosphorylation as previously described. Data represent mean ± SEM (n = 3). *$p < 0.05$ and ***$p < 0.0005$. (D) Left: Immunoblotting of signaling proteins in control and DKO iPSCs grown for 24 hours in basal media that were stimulated with 100 nM insulin for 15 min; β-actin served as a loading control. Right: Quantification of phosphorylation as previously described. Data represent mean ± SEM (n = 3). *$p < 0.05$, **$p < 0.005$, and ***$p < 0.0005$. (E) Left: Immunoblotting of signaling proteins in control and DKO iPSCs grown for 24 hours in basal media that were stimulated with 100 units/mL of LIF for 15 min; β-actin served as a loading control. Right: Quantification of phosphorylation as previously described. Data represent mean ± SEM (n = 3). *$p < 0.05$, **$p < 0.005$, and ***$p < 0.0005$.

To assess the differentiation potential in vivo, we injected similar numbers (1 million cells) of control or DKO iPSCs either intramuscularly or subcutaneously into independent NOD-SCID mice and observed them for 4 weeks. Both groups exhibited teratomas within this time period; the average teratoma area was not statistically different between the groups (control iPSCs, 2.75 cm³ vs DKO iPSCs, 1.84 cm³) (Figure 1F). Hematoxylin and eosin staining and immunohistochemistry of sections of the teratomas revealed the presence of all 3 germ layers in both groups (Figure 1G). Interestingly, teratomas derived from DKO iPSCs exhibited a preponderance of primitive neuroectodermal tissue, with multifocal rosette formation and abundant atypical mitotic figures (Figure 1H). This tissue was similar in appearance to primitive neuroectodermal tumor tissue [33]. These data suggest that iPSCs devoid of insulin/IGF-1 receptors show a perturbation in differentiation with a preference toward the formation of neuroectodermal tissue.

4.2. RNA-seq analyses revealed differential regulation of genes/pathways related to pluripotency, development, metabolism, and apoptosis

To gain insight into the molecular differences between the groups, we undertook next generation RNA-seq of control (n = 3) vs DKO (n = 4) iPSCs at the basal level. Identification of the top 50 most differentially regulated genes between the groups (Figure 2A, B, and Table 1) by Volcano plot analyses confirmed that IR and IGF1R were among the most downregulated in DKO iPSCs (Figure 2C). Interestingly, *Stat3* and *Socs3* were found to be upregulated, as was their target *Lefty2* [34]. *Lefty2* expression in mouse ESCs has been implicated in the maintenance of pluripotency [35]. Honing in on pluripotency markers, DKOs showed statistically significant upregulation of mouse ESC pluripotent marker *Tfcp2l1* (another target of *Stat3*) [36]. These data indicate that DKO of IR and IGF1R may promote stem cell pluripotency by allowing increased expression of pluripotency genes that are regulated in part by *Stat3*.

To explore the differential pathway regulation between control and DKO iPSCs, we performed gene ontology enrichment analysis. It showed that, compared to controls, DKO iPSCs exhibited downregulation of pathways implicated in cell differentiation (Notch1), DNA synthesis, protein translation, longevity, and cell-cycle arrest. Upregulated pathways included those important in myogenesis, DNA repair, and cytokine signaling (Figs. 2D, 2E, S2A, and S2B and Tables 2 and 3). This analysis suggests that there is direct involvement of IR/IGF1R-mediated signaling in cell differentiation, growth, and development. Interestingly, transcription factor analysis showed that DKOs compared to controls had predominant upregulation of the *E2F* family and caspase pathways and downregulation of the Fas pathway (Figs. S2C and S2D and Tables 4 and 5).
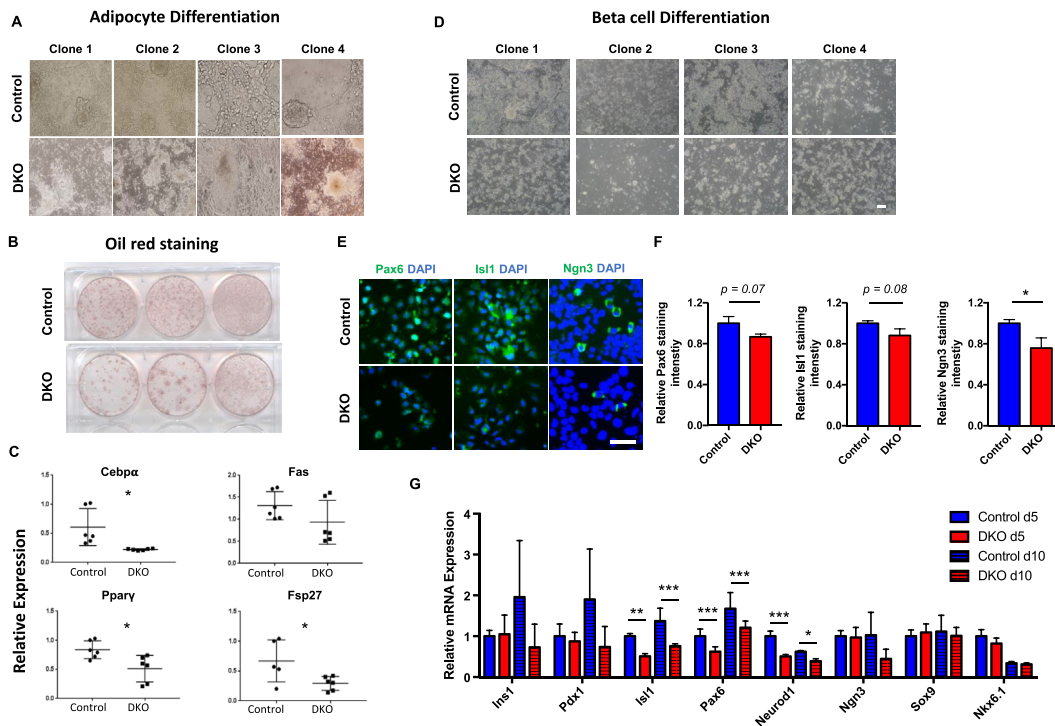
Figure 4: Adipocyte and pancreatic endocrine progenitor cell differentiation were deregulated in DKO iPSCs. (A) Representative morphological images of control and DKO differentiating adipocytes on day 28. (B) Representative Oil Red O staining images of control and DKO differentiating adipocytes on day 28. (C) Relative gene expression analyzed by qRT-PCR of *Cebpα*, *Fas*, *Pparγ*, and *Fsp27* in control and DKO differentiating adipocytes on day 28. Gene expression levels were normalized to β-actin. Data represent mean ± SEM (n = 3). Statistical analysis by two-way ANOVA with Tukey's multiple comparisons test. *p < 0.05. (D) Representative morphological images of control and DKO differentiating beta-like cells on day 10. (E) Representative images of control and DKO cells (day 10) immunostained for markers of pancreatic endocrine progenitor cells (Pax6, Isl1, and Ngn3 in green and nuclei stained with DAPI in blue). Scale bar is 200 μm. (F) Quantification of staining intensity by ImageJ. Data are represented as mean ± SEM (n = 4 clones/group in triplicate). Statistical analysis by unpaired *t*-test with Welch's correction. *p < 0.05. (G) Relative gene expression analyzed by qRT-PCR of *Ins1*, *Pdx1*, *Isl1*, *Pax6*, *NeuroD1*, *Ngn3*, *Sox9*, and *Nkx6.1* in control and DKO pancreatic endocrine progenitor cells on days 5 and 10 of differentiation. Gene expression was normalized to β-actin and DKO expression was normalized to controls using the comparative threshold cycle (ΔΔCT) method. Data are represented as mean ± SEM (n = 4 clones/group in triplicate). Statistical analysis by two-way ANOVA with Tukey's multiple comparisons test. *p < 0.05, **p < 0.005, and ***p < 0.0001.

4.3. Signaling pathway analyses demonstrated differential regulation of key pluripotency pathways in DKOs

To analyze the consequences of knocking out both insulin and IGF-1 receptors in iPSCs, we examined their downstream signaling signatures. We first cultured iPSCs in regular media to assess the expression of signaling proteins in an unstimulated state. Both control and DKO iPSCs showed mTOR, AKT, and ERK protein phosphorylation in the basal state (Figure 3A). Phosphorylation of mTOR in the DKOs was significantly lower than controls (28% of controls; p < 0.05). Total mTOR and AKT protein levels in DKOs were also lower (31% and 59% of controls, respectively; p < 0.05) (Figure 3B).

In the next set of experiments, we stimulated iPSCs with insulin or IGF-1 to more clearly elucidate the differences in signaling pathways between the two groups. As expected, stimulation of DKO iPSCs with exogenous IGF-1 (100 nM for 15 min) did not lead to significant phosphorylation of downstream signaling proteins AKT and ERK (98% and 78% less than controls, respectively); mTOR phosphorylation was similar between the groups. Interestingly, STAT3 phosphorylation in the basal state was already evident in DKOs and increased 11-fold after treatment compared to controls (Figure 3C). When cells were stimulated with insulin (100 nM for 15 min), AKT phosphorylation in DKOs was also 98% lower than controls while ERK and mTOR phosphorylation were similar between the groups. We again observed an interesting pattern with STAT3 phosphorylation. Only DKOs showed STAT3 phosphorylation in the basal state; furthermore, this increased 3-fold with treatment as compared to controls (Figure 3D).

We used leukemia inhibitory factor (LIF) (100 unit/mL for 15 min) to examine the effects of a potent regulator of pluripotency in the two groups of iPSCs. Compared to controls, AKT and ERK phosphorylation were 44% and 26% lower in DKOs, respectively. While mTOR phosphorylation was similar between the groups, STAT3 phosphorylation was 1.5-fold greater in DKOs as compared to controls (p < 0.005) (Figure 3E). Given that STAT3 is downstream of the LIF receptor (LIFR), we assessed LIFR protein levels in both control and DKO iPSCs; there was no difference in protein expression between the 2 groups (data not shown). These data are in contrast to what was noted in day 10 embryoid bodies; in those cells, we did not observe any difference in the AKT/ERK/mTOR/STAT3 pathways (Figures. S3A and 3B).

The upregulation of STAT3 protein in DKO iPSCs in the basal state and after stimulation with insulin, IGF-1, or LIF corroborates our RNA-seq findings of increased STAT3 RNA expression and increased expression of STAT3 targets.

4.4. DKO iPSCs exhibited dysregulated expression of markers of development of all three lineages

To understand the role of these receptors in differentiation, we performed directed differentiation of control and DKO iPSCs toward all three lineages. We used a previously described protocol [25,38] to differentiate control and DKO iPSCs toward the ectodermal lineage. On

day 10 we performed immunocytochemistry on differentiated neuronal-like cells using antibodies directed against nestin (an early neuron marker), N-cadherin (an early to immature neuron marker), beta-III-tubulin (an immature neuron marker), or synaptophysin (a mature neuron marker). Both control and DKO cells showed similar immunostaining for all of the markers on day 10 (Figure S4A) and morphological analyses revealed neuronal-like cells in both groups (Figure S4B). We then assessed the protein abundance of neuronal Sox2, nestin, N-cadherin, and synaptophysin in control and DKO neuronal-like cells via Western blotting densitometry analysis (Figures. S4C and D). The protein levels of nestin and N-cadherin (early neuronal markers) were increased in DKO neuronal-like cells, suggesting an interruption in neuronal differentiation [39,40].

We next assessed the significance of IR/IGF1R-mediated signaling in adipogenesis, a candidate cell type from the mesodermal lineage. The iPSCs from both groups were differentiated into pre-adipocytes over 28 days using a modified step-by-step protocol [41]. Morphological analyses of the iPSCs on day 27 of differentiation showed decreased adipocytes derived from the DKO group as compared to controls (Figure 4A). This limited ability to differentiate was supported by Oil Red O staining showing a reduced number of droplets in the DKO adipocytes compared to controls (Figure 4B). Consistently, the expression levels of *Cebpα, Fas, Pparγ, and Fsp27* were significantly downregulated in the adipocytes differentiated from DKO iPSCs (Figure 4C). We did not detect the expression of *Lep* and *Ucp1*, probably due to the early stage of differentiation [42] (data not shown). These findings agree with results from [43], who reported that adipocyte-specific knockout of both of these receptors in mice led to a paucity of brown and white adipose tissue.

We undertook directed differentiation toward the endodermal lineage using a protocol to derive pancreatic endocrine progenitors [25,44,45]. Pancreatic endocrine progenitor cells were analyzed at an early stage (day 5) and late stage (day 10) of differentiation (Figure 4D). There was a significant increase in apoptosis in DKO cells as compared to controls in both the early and late stages (Figures. S4E and F). Immunostaining analysis showed downregulation of Pax6, Isl1, and Ngn3 in DKO cells during the late stages of pancreatic endocrine progenitor cell differentiation (Figure 4E, F). Gene expression analysis revealed significant decreases in the endodermal progenitor transcription factors *Isl1*, *Pax6*, and *Neurod1* in DKO cells on days 5 and 10. Expression levels of the beta cell markers *Ins1* and *Pdx1* and the endodermal progenitor marker *Ngn3* tended to be lower in DKOs compared to control cells during the later stages of differentiation (Figure 4G).

These studies suggest that IR and IGF1R are important for normal differentiation of mouse iPSCs and necessary for cell survival when differentiation is directed toward an endodermal lineage.

5. DISCUSSION

Insulin/IGF-1 receptors and their downstream signaling proteins serve important roles in cellular growth, proliferation, and metabolism during all stages of development and in adulthood. In the present study, we sought to understand their combined role in pluripotency and lineage development of stem cells. Our results indicate that these receptors are necessary for somatic cell transformation into iPSCs and are required for normal lineage development.

One consistent finding in our studies was enhanced activation and expression of STAT3 in the DKO iPSCs compared to controls in the basal and stimulated states. In contrast, in our previous study we observed that phosphorylation of STAT3 was reduced in iPSCs that only lacked the IR [25]. One conclusion from these two studies is that

IGF1R is an important contributor to regulating STAT3 signaling in the pluripotent state. STAT3, a transcription factor downstream of the LIFR and its heterodimer, GPR130F, have been shown to regulate a variety of genes including those implicated in pluripotency such as Sox2, Klf4, Myc, and Bcl3 and to cooperate with Nanog to maintain pluripotency [46,47]. Constitutively active STAT3 can sustain stem cell self-renewal, even in the absence of LIF, and transfection of a dominant negative STAT3 leads to mouse ESC differentiation [47—49]. Hyperactive STAT3 has been shown to induce differentiation of mouse ESCs to trophectoderm [50]. The regulation of STAT3 is mediated in part by suppressors of cytokine signaling (SOCS) and protein inhibitors of activated STAT (PIAS), two proteins that lead to STAT3 dephosphorylation. In this context it is worth noting that IGF1R has been shown to interact with SOCS protein in vitro [51,52]. Thus, we speculate that the upregulation of the JAK/STAT pathway in DKO iPSCs is able to abrogate the potentially deleterious effects consequent to the absence of IR/IGF-1 receptors. Whether the increased STAT3 expression in DKO iPSCs directly contributes to the appearance of primitive neuroectodermal tissue in teratomas requires further investigation.

To investigate the role of IR/IGF-1 receptors in lineage development we directly differentiated control and DKO iPSCs into neuronal-like cells (ectoderm), adipocytes (mesoderm), or pancreas endocrine progenitor cells (endoderm). Regarding the ectodermal lineage, DKO iPSCs showed upregulation of early neuronal markers nestin and N-cadherin on day 10, suggesting an inability to normally differentiate into mature functional neurons [39,40]. In contrast, a similar differentiation approach of IR KOs in our previous study showed an upregulation of other neuronal markers *Pax6*, *Tubb3*, *Asci*, and *Oligo2* but not nestin or N-cadherin [25]. These data suggest that the presence of IGF1R is necessary to regulate neuronal markers during development. However, the precise contributions of nestin and N-cadherin to the development of mature and functional neurons warrant further investigation.

When directed to differentiate toward the mesodermal lineage, DKO iPSCs showed reduced adipogenesis along with significantly reduced expression of lipogenesis markers *Fas*, *Pparγ*, *Fsp27*, and *Cebpα*. Fas is a lipogenic enzyme while Fsp27 is involved in unilocular lipid droplet and adipocyte formation [53]. *Cebpα* is reported to play a developmental role in adipogenesis [54]. Similarly, our IR KO study showed not only downregulation of *Fas*, *Pparγ*, *Fsp27*, and *Cebpα* but also other adipocyte markers including *Acc*, *Cebpβ*, and *Fabp4* [25]. Curiously, we did not observe differences in the expression of mature adipocyte markers such as leptin and adiponectin in our current or previous studies.

DKO iPSCs displayed a poor ability to differentiate toward pancreatic endocrine progenitors as shown by a reduced expression of key pancreatic cell developmental markers *Isl1*, *Pax6*, and *NeuroD1* [55,56]. Furthermore, the protein abundance of Ngn3 was reduced in DKO differentiated pancreatic endocrine progenitor cells. Insulin1 (*Ins1*) expression was similar between the groups in the early stage of differentiation and tended to decrease in the later stages. These results are consistent with our previous observations that knocking out IR in the pluripotent stage impacts pancreatic endocrine progenitor and beta-like cell development by regulating *Ngn3*, *Isl1*, and *Sox9* [25]. Of note, knocking out insulin and/or IGF-1 receptors in adult hormonal cells leads to different phenotypes, indicating the context-dependent roles of these receptors. For example, tissue-specific IR KO in pancreatic beta cells leads to defects in insulin secretion and an age-dependent decrease in beta cell mass [57], while beta cell-specific IGF1R KO [58,59] manifests as a secretory defect without alteration of beta cell mass or development.

Brief Communication

DKO iPSCs differentiated to form primitive neuroectodermal tissue in teratomas but exhibited increased apoptosis when they underwent directed differentiation into adipocytes and pancreatic endocrine progenitor cells. Both of these processes may be due to upregulation of the E2F1 pathway, a central player involved in cell cycle progression, DNA damage response, and apoptosis. Indeed, overexpression of E2F1 has been shown to induce tumor formation in rodent primary cells and transgenic mice [60] and has been linked to apoptosis [61].

In summary, the present study reveals the developmental role of IR/IGF1R signaling in neuronal, adipocyte, and pancreatic endocrine progenitor cell differentiation. Cells lacking these receptors in the pluripotent stage stall at earlier stages of differentiation and are unable to fully mature. iPSCs lacking insulin and IGF1 receptors compensate by upregulating the JAK/STAT3 pathway. Further studies are warranted to explore the relevance of IR/IGF1R in modulating the E2F1-apoptotic pathway during development.

AUTHOR CONTRIBUTIONS

E.R.O. and M.K.G. conceived the idea. E.R.O. designed and performed the experiments, analyzed the data, and wrote the manuscript. M.K.G. contributed to generation and maintenance of iPSCs, conducted the experiments, and assisted with the data analysis and discussion. S.K. performed the experiments and assisted with the data analysis. P.G. conducted the experiments and edited the manuscript. J.H. contributed to the immunohistochemistry. K.D. and B.S. contributed to the in vitro cell culture experiments. J.L. contributed to the teratoma analysis. R.N.K. conceived the idea, designed the experiments, contributed to discussions, edited the manuscript, and is the guarantor of this work. All authors read and approved the manuscript.

ACKNOWLEDGMENTS

CONFLICTS OF INTEREST

None declared.

APPENDIX A. SUPPLEMENTARY DATA

Supplementary data to this article can be found online at https://doi.org/10.1016/j.molmet.2021.101164.

REFERENCES

[1] Haeusler, R.A., McGraw, T.E., Accili, D., 2018. Biochemical and cellular properties of insulin receptor signalling. Nature Reviews. Molecular Cell Biology 19:31—44.

[2] Kitamura, T., Nakae, J., Kitamura, Y., Kido, Y., Biggs 3rd, W.H., Wright, C.V., et al., 2002. The forkhead transcription factor Foxo1 links insulin signaling to Pdx1 regulation of pancreatic beta cell growth. Journal of Clinical Investigation 110:1839—1847.

[3] Stewart, C.E., Rotwein, P., 1996. Growth, differentiation, and survival: multiple physiological functions for insulin-like growth factors. Physiological Reviews 76:1005—1026.

[4] Lighten, A.D., Hardy, K., Winston, R.M., Moore, G.E., 1997. Expression of mRNA for the insulin-like growth factors and their receptors in human preimplantation embryos. Molecular Reproduction and Development 47:134—139.

[5] Piper, K., Brickwood, S., Turnpenny, L.W., Cameron, I.T., Ball, S.G., Wilson, D.I., et al., 2004. Beta cell differentiation during early human pancreas development. Journal of Endocrinology 181:11—23.

[6] Accili, D., Drago, J., Lee, E.J., Johnson, M.D., Cool, M.H., Salvatore, P., et al., 1996. Early neonatal death in mice homozygous for a null allele of the insulin receptor gene. Nature Genetics 12:106—109.

[7] Liu, J.P., Baker, J., Perkins, A.S., Robertson, E.J., Efstratiadis, A., 1993. Mice carrying null mutations of the genes encoding insulin-like growth factor I (Igf-1) and type 1 IGF receptor (Igf1r). Cell 75:59—72.

[8] Louvi, A., Accili, D., Efstratiadis, A., 1997. Growth-promoting interaction of IGF-II with the insulin receptor during mouse embryonic development. Developmental Biology 189:33—48.

[9] Taniguchi, C.M., Emanuelli, B., Kahn, C.R., 2006. Critical nodes in signalling pathways: insights into insulin action. Nature Reviews. Molecular Cell Biology 7:85—96.

[10] White, M.F., 2002. IRS proteins and the common path to diabetes. American Journal of Physiology. Endocrinology and Metabolism 283:E413—E422.

[11] Takahashi, T., Fukuda, K., Pan, J., Kodama, H., Sano, M., Makino, S., et al., 1999. Characterization of insulin-like growth factor-1-induced activation of the JAK/STAT pathway in rat cardiomyocytes. Circulation Research 85:884—891.

[12] Zong, C.S., Chan, J., Levy, D.E., Horvath, C., Sadowski, H.B., Wang, L.H., 2000. Mechanism of STAT3 activation by insulin-like growth factor I receptor. Journal of Biological Chemistry 275:15099—15105.

[13] Alva, J.A., Lee, G.E., Escobar, E.E., Pyle, A.D., 2011. Phosphatase and tensin homolog regulates the pluripotent state and lineage fate choice in human embryonic stem cells. Stem Cells 29:1952—1962.

[14] Armstrong, L., Hughes, O., Yung, S., Hyslop, L., Stewart, R., Wappler, I., et al., 2006. The role of PI3K/AKT, MAPK/ERK and NFkappabeta signalling in the maintenance of human embryonic stem cell pluripotency and viability highlighted by transcriptional profiling and functional analysis. Human Molecular Genetics 15:1894—1913.

[15] Jirmanova, L., Afanassieff, M., Gobert-Gosse, S., Markossian, S., Savatier, P., 2002. Differential contributions of ERK and PI3-kinase to the regulation of cyclin D1 expression and to the control of the G1/S transition in mouse embryonic stem cells. Oncogene 21:5515—5528.

[16] McLean, A.B., D'Amour, K.A., Jones, K.L., Krishnamoorthy, M., Kulik, M.J., Reynolds, D.M., et al., 2007. Activin a efficiently specifies definitive endoderm from human embryonic stem cells only when phosphatidylinositol 3-kinase signaling is suppressed. Stem Cells 25:29—38.

[17] Paling, N.R., Wheadon, H., Bone, H.K., Welham, M.J., 2004. Regulation of embryonic stem cell self-renewal by phosphoinositide 3-kinase-dependent signaling. Journal of Biological Chemistry 279:48063—48070.

[18] Greber, B., Coulon, P., Zhang, M., Moritz, S., Frank, S., Muller-Molina, A.J., et al., 2011. FGF signalling inhibits neural induction in human embryonic stem cells. The EMBO Journal 30:4874—4884.

[19] Chen, H., Guo, R., Zhang, Q., Guo, H., Yang, M., Wu, Z., et al., 2015. Erk signaling is indispensable for genomic stability and self-renewal of mouse embryonic stem cells. In: Proceedings of the National Academy of Sciences of the United States of America 112. p. E5936—43.

[20] Ying, Q.L., Wray, J., Nichols, J., Batlle-Morera, L., Doble, B., Woodgett, J., et al., 2008. The ground state of embryonic stem cell self-renewal. Nature 453:519—523.

[21] Anderson, K.G.V., Hamilton, W.B., Roske, F.V., Azad, A., Knudsen, T.E., Canham, M.A., et al., 2017. Insulin fine-tunes self-renewal pathways governing naive pluripotency and extra-embryonic endoderm. Nature Cell Biology 19:1164—1177.

[22] Hsu, H.J., Drummond-Barbosa, D., 2009. Insulin levels control female germline stem cell maintenance via the niche in Drosophila. In: Proceedings of the National Academy of Sciences of the United States of America 106. p. 1117—21.

[23] LaFever, L., Drummond-Barbosa, D., 2005. Direct control of germline stem cell division and cyst growth by neural insulin in Drosophila. Science 309: 1071—1073.

[24] Ziegler, A.N., Schneider, J.S., Qin, M., Tyler, W.A., Pintar, J.E., Fraidenraich, D., et al., 2012. IGF-II promotes stemness of neural restricted precursors. Stem Cells 30:1265—1276.

[25] Gupta, M.K., De Jesus, D.F., Kahraman, S., Valdez, I.A., Shamsi, F., Yi, L., et al., 2018. Insulin receptor-mediated signaling regulates pluripotency markers and lineage differentiation. Molecular metabolism 18:153—163.

[26] Toyoshima, Y., Monson, C., Duan, C., Wu, Y., Gao, C., Yakar, S., et al., 2008. The role of insulin receptor signaling in zebrafish embryogenesis. Endocrinology 149:5996—6005.

[27] Bendall, S.C., Stewart, M.H., Menendez, P., George, D., Vijayaragavan, K., Werbowetski-Ogilvie, T., et al., 2007. IGF and FGF cooperatively establish the regulatory stem cell niche of pluripotent human cells in vitro. Nature 448: 1015—1021.

[28] Wang, L., Schulz, T.C., Sherrer, E.S., Dauphin, D.S., Shin, S., Nelson, A.M., et al., 2007. Self-renewal of human embryonic stem cells requires insulin-like growth factor-1 receptor and ERBB2 receptor signaling. Blood 110:4111—4119.

[29] Waraky, A., Aleem, E., Larsson, O., 2016. Downregulation of IGF-1 receptor occurs after hepatic linage commitment during hepatocyte differentiation from human embryonic stem cells. Biochemical and Biophysical Research Communications 478:1575—1581.

[30] Chaker, Z., Aid, S., Berry, H., Holzenberger, M., 2015. Suppression of IGF-I signals in neural stem cells enhances neurogenesis and olfactory function during aging. Aging Cell 14:847—856.

[31] Gong, H., Wang, X., Wang, L., Liu, Y., Wang, J., Lv, Q., et al., 2017. Inhibition of IGF-1 receptor kinase blocks the differentiation into cardiomyocyte-like cells of BMSCs induced by IGF-1. Molecular Medicine Reports 16:787—793.

[32] Takahashi, K., Yamanaka, S., 2006. Induction of pluripotent stem cells from mouse embryonic and adult fibroblast cultures by defined factors. Cell 126: 663—676.

[33] Tan, Y., Zhang, H., Ma, G.L., Xiao, E.H., Wang, X.C., 2014. Peripheral primitive neuroectodermal tumor: dynamic CT, MRI and clinicopathological characteristics–analysis of 36 cases and review of the literature. Oncotarget 5:12968—12977.

[34] Cinelli, P., Casanova, E.A., Uhlig, S., Lochmatter, P., Matsuda, T., Yokota, T., et al., 2008. Expression profiling in transgenic FVB/N embryonic stem cells overexpressing STAT3. BMC Developmental Biology 8:57.

[35] Kim, D.K., Cha, Y., Ahn, H.J., Kim, G., Park, K.S., 2014. Lefty1 and lefty2 control the balance between self-renewal and pluripotent differentiation of mouse embryonic stem cells. Stem Cells and Development 23:457—466.

[36] Martello, G., Bertone, P., Smith, A., 2013. Identification of the missing pluripotency mediator downstream of leukaemia inhibitory factor. The EMBO Journal 32:2561—2574.

[38] Ying, Q.L., Stavridis, M., Griffiths, D., Li, M., Smith, A., 2003. Conversion of embryonic stem cells into neuroectodermal precursors in adherent monoculture. Nature Biotechnology 21:183—186.

[39] Bott, C.J., Johnson, C.G., Yap, C.C., Dwyer, N.D., Litwa, K.A., Winckler, B., 2019. Nestin in immature embryonic neurons affects axon growth cone morphology and Semaphorin3a sensitivity. Molecular Biology of the Cell 30: 1214—1229.

[40] Paulson, A.F., Prasad, M.S., Thuringer, A.H., Manzerra, P., 2014. Regulation of cadherin expression in nervous system development. Cell Adhesion & Migration 8:19—28.

[41] Cuaranta-Monroy, I., Simandi, Z., Kolostyak, Z., Doan-Xuan, Q.M., Poliska, S., Horvath, A., et al., 2014. Highly efficient differentiation of embryonic stem cells into adipocytes by ascorbic acid. Stem Cell Research 13:88—97.

[42] Basse, A.L., Dixen, K., Yadav, R., Tygesen, M.P., Qvortrup, K., Kristiansen, K., et al., 2015. Global gene expression profiling of brown to white adipose tissue transformation in sheep reveals novel transcriptional components linked to adipose remodeling. BMC Genomics 16:215.

[43] Boucher, J., Softic, S., El Ouaamari, A., Krumpoch, M.T., Kleinridders, A., Kulkarni, R.N., et al., 2016. Differential roles of insulin and IGF-1 receptors in adipose tissue development and function. Diabetes 65:2201—2213.

[44] Gu, G., Dubauskaite, J., Melton, D.A., 2002. Direct evidence for the pancreatic lineage: NGN3+ cells are islet progenitors and are distinct from duct progenitors. Development 129:2447—2457.

[45] Liu, S.H., Lee, L.T., 2012. Efficient differentiation of mouse embryonic stem cells into insulin-producing cells. Experimental Diabetes Research 2012: 201295.

[46] Cartwright, P., McLean, C., Sheppard, A., Rivett, D., Jones, K., Dalton, S., 2005. LIF/STAT3 controls ES cell self-renewal and pluripotency by a Myc-dependent mechanism. Development 132:885—896.

[47] Hall, J., Guo, G., Wray, J., Eyres, I., Nichols, J., Grotewold, L., et al., 2009. Oct4 and LIF/Stat3 additively induce Kruppel factors to sustain embryonic stem cell self-renewal. Cell stem cell 5:597—609.

[48] Matsuda, T., Nakamura, T., Nakao, K., Arai, T., Katsuki, M., Heike, T., et al., 1999. STAT3 activation is sufficient to maintain an undifferentiated state of mouse embryonic stem cells. The EMBO Journal 18:4261—4269.

[49] Niwa, H., Burdon, T., Chambers, I., Smith, A., 1998. Self-renewal of pluripotent embryonic stem cells is mediated via activation of STAT3. Genes & Development 12:2048—2060.

[50] Tai, C.I., Schulze, E.N., Ying, Q.L., 2014. Stat3 signaling regulates embryonic stem cell fate in a dose-dependent manner. Biology open 3:958—965.

[51] Dey, B.R., Spence, S.L., Nissley, P., Furlanetto, R.W., 1998. Interaction of human suppressor of cytokine signaling (SOCS)-2 with the insulin-like growth factor-I receptor. Journal of Biological Chemistry 273:24095—24101.

[52] Dhar, K., Rakesh, K., Pankajakshan, D., Agrawal, D.K., 2013. SOCS3 promotor hypermethylation and STAT3-NF-kappaB interaction downregulate SOCS3 expression in human coronary artery smooth muscle cells. American Journal of Physiology. Heart and Circulatory Physiology 304:H776—H785.

[53] Zhou, L., Park, S.Y., Xu, L., Xia, X., Ye, J., Su, L., et al., 2015. Insulin resistance and white adipose tissue inflammation are uncoupled in energetically challenged Fsp27-deficient mice. Nature Communications 6:5949.

[54] Darlington, G.J., Ross, S.E., MacDougald, O.A., 1998. The role of C/EBP genes in adipocyte differentiation. Journal of Biological Chemistry 273:30057—30060.

[55] Ediger, B.N., Du, A., Liu, J., Hunter, C.S., Walp, E.R., Schug, J., et al., 2014. Islet-1 Is essential for pancreatic beta-cell function. Diabetes 63:4206—4217.

[56] Gradwohl, G., Dierich, A., LeMeur, M., Guillemot, F., 2000. neurogenin3 is required for the development of the four endocrine cell lineages of the pancreas. In: Proceedings of the National Academy of Sciences of the United States of America 97. p. 1607—11.

[57] Kulkarni, R.N., Bruning, J.C., Winnay, J.N., Postic, C., Magnuson, M.A., Kahn, C.R., 1999. Tissue-specific knockout of the insulin receptor in pancreatic beta cells creates an insulin secretory defect similar to that in type 2 diabetes. Cell 96:329—339.

[58] Kulkarni, R.N., Holzenberger, M., Shih, D.Q., Ozcan, U., Stoffel, M., Magnuson, M.A., et al., 2002. beta-cell-specific deletion of the Igf1 receptor leads to hyperinsulinemia and glucose intolerance but does not alter beta-cell mass. Nature Genetics 31:111—115.

[59] Xuan, S., Kitamura, T., Nakae, J., Politi, K., Kido, Y., Fisher, P.E., et al., 2002. Defective insulin secretion in pancreatic beta cells lacking type 1 IGF receptor. Journal of Clinical Investigation 110:1011—1019.

[60] Olson, M.V., Johnson, D.G., Jiang, H., Xu, J., Alonso, M.M., Aldape, K.D., et al., 2007. Transgenic E2F1 expression in the mouse brain induces a human-like bimodal pattern of tumors. Cancer Research 67:4005—4009.

[61] Wu, X., Levine, A.J., 1994. p53 and E2F-1 cooperate to mediate apoptosis. In: Proceedings of the National Academy of Sciences of the United States of America 91. p. 3602—6.

[62] Shirakawa, J., Fernandez, M., Takatani, T., El Ouaamari, A., Jungtrakoon, P., Okawa, E.R., et al., 2017. Insulin signaling regulates the FoxM1/PLK1/CENP-A pathway to promote adaptive pancreatic beta cell proliferation. Cell Metabolism 25:868—882 e865.